



# Journal of Applied and Computational Mechanics



## Research Paper

# Bio-Convection Flow of Sutterby Nanofluid with Motile Microbes on Stretchable Sheet: Exponentially Varying Viscosity

Galal M. Moatimid<sup>✉</sup>, Nasser S. Elgazery<sup>✉</sup>, Mona A.A. Mohamed<sup>✉</sup>, Khaled Elagamy<sup>✉</sup>

Department of Mathematics, Faculty of Education, Ain Shams University, Roxy, Heliopolis:11566, Cairo, Egypt  
Email: gal\_moa@edu.asu.edu.eg (G.M.M.); nasersaleh@edu.asu.edu.eg (N.S.E.); monaali@edu.asu.edu.eg (M.A.A.M.); khaledagami@edu.asu.edu.eg (K.E.)

Received December 10 2023; Revised February 18 2024; Accepted for publication February 19 2024.

Corresponding author: Mona A.A. Mohamed (monaali@edu.asu.edu.eg)

© 2024 Published by Shahid Chamran University of Ahvaz

**Abstract.** The present work studies the bio-convection movement of an incompressible non-Newtonian Sutterby liquid on a stretchable surface in the existence of both nanomaterials and microbes. The liquid flows throughout a leaky region and is affected by a homogeneous vertical magnetic field. The energy spread is established by Ohmic and non-Newtonian dissipations in addition to an exponentially-space heat source, while the nanomaterials transmission is reachable with chemical reaction. The physical configuration is covered by force, temperature, nano-volume fractions, and microbes' formulae together with the appropriate border criteria. The novel aspect of this work is motivated due to its consideration of the exponential distribution of viscosity with temperature, concentration of microorganisms, and nanoparticles. Furthermore, the involvement of microbes in the flow across a stretched surface added another innovative feature, in light of its wide application range. The foremost format of nonlinear partial differential formulae is transformed into ordinary ones providing suitable match converters. These formulae are scrutinized by the fourth-order Runge-Kutta numerical technique with the support of shooting criteria. Consequently, arithmetical and graphical foundations of the objective distributions are achieved. The conclusions are examined, and significant results are summarized. Several important physiognomies are completed from the outcomes. The heat profile improves the efficient factors, which is an excellent rule that may be employed in various implications. Microbes' accumulation is found to increase with the increase of viscosity variation, whereas it decreases with the growth of Peclet, Lewis numbers, and the bio convection constants. Such findings may be useful in expecting the behavior of these microscopic organisms through similar flows.

**Keywords:** Non-Newtonian Sutterby liquid; Microorganisms; Permeable medium; Variable Viscosity; Exponentially-space heat source.

## 1. Introduction

There is a wide range of applications of nanomaterials, including oil extraction, heat storage devices, cooling systems, fluid construction, oil recovery, engineering and manufacturing, and biotechnology. Many researchers were interested in the real-world applications of non-Newtonian Sutterby liquid (NSF) in various technical disciplines and engineering, together with gas turbines, polymer fabrication, control generators, paper making, cable representation, glass material, are mention a few. The flow of Magnetohydrodynamics (MHD) of NSF over a stretching cylinder was studied in relation to the impacts of energy rays, stratification, and Joule dispersion [1]. The main finding of this study was that the radiation boosts the system's temperature while changing thermal conductivity causes it to drop. Biologically inspired propulsion systems were becoming progressively significant to the engineering domain. The influence of heterogeneous-homogeneous processes on the temperature was theoretically investigated, and temperature transmission for incompressible NSF was examined [2]. The applications of this work in biological processes and biomedical engineering, such as electromagnetic peristaltic micro pumps, were numerous. In addition to the existence of heat rays and MHD, the NSF and the problem of temperature transfer over a leaky movable surface were examined [3]. The characteristics of heat transmission and fluid flow close to the stagnation zone were considered. The revolving flexible disc that caused the NSF to flow was examined [4]. The heat source, chemical reaction, and the effects of magnetic field (MF) were considered. The effects of the various factors on concentration, energy, and speed were explained. A linearly stretchy sheet was used to deform the NSF, and the results were carefully examined [5]. To investigate the characteristics of electrically conducting fluid, inclined MF was added. To further clarify the heat transfer, the phenomenon of thermal stratification was applied to a horizontal sheet. For greater thermal conductivity parameters, it was exposed that the temperature increased, while the speed was decreased with the enhancement of the fluid parameter. The Galerkin finite element technique was used to solve a complex set of mathematical models resulting from the rheology of the NSF [6]. A stretching/shrinking wedge is affected by the bio convection as well as thermal radiation, and an activation energy-based numerical model for the NSF was exposed [7]. Tables and graphs showed the arithmetical results of the profiles of temperature, speed, volume fractions, and microorganism diffusions due to different scheming



contributors. An incompressible micropolar NSF's peristaltic transport was studied [8]. Within the two-measurement symmetric perpendicular tube, mass and heat transmission were measured. In addition to heat rays, couple stress, chemical reaction, Ohm's dispersion, temperature creation, Dufour, Soret, and Hall contributions, the system was impacted by a high MF. Under the effect of zero mass fluctuation and temperature convection circumstances, the temperature transfer features of quadratic temperature rays and quadratic convection unbalanced stagnation position stream of electromagnetic NSF on a whirling sphere were studied [9]. The results demonstrated that the increases in the MF, electric field (EF), and the quadratic radiation parameter enhance the NSF's heat profile. The motile gyrotactic microorganisms were involved in the flow of the NSF that carried minute particles, and the induced MF was investigated [10]. The aforementioned works explore the NSF because of its practical uses in many technical parts and productions.

One area of practical microbiology is called "industrial microbiology", where microorganisms are employed to make essential goods like food products, biological transformation, energy production, deal with organic and industrial wastes, production of microbial biomass for food and feeding, and the production of bio-control agents. Moving microorganisms performed in an incompressible MHD nano liquid according to the Jeffrey prototype was studied [11]. The symmetrical movement with peristalsis of microbes in a Rabinowitsch liquid was examined [12]. It was supposed that the compactness with the gravity effect expression in the Boussinesq approximation (BA) was a linear function of concentrations and heat. The peristalsis-driven flow in a horizontal channel advanced simultaneously with the deposition of thermophoretic particles. A modified version of Darcy's law was used to study the pulsatile motion of an incompressible Williamson MHD nanofluid in a leaky region in the presence of motile microorganisms [13]. The roles bacteria, fungi, and nanoparticles play in the application of pulsatile drive flow were highlighted. A time-periodic and bioconvection BC-equipped annular rotating tube was used to study the Walters' B liquid incompressible flow [14]. An analytical solving method was considered for the given flow via a porous material with a uniform perpendicular MF effect. Following the Carreau prototype, the MHD free convective action with peristalsis of a non-Newtonian nanofluid was studied in conjunction with the movement of microorganisms [15]. Motile microorganisms were connected to the movement within a permeable medium utilizing a modified Darcy law [16]. The flow is taken through a boundary layer encircled a porous vertical surface that expands in size. The rate of heat, mass, and motile microbe movements in the convective flow of the MHD second-grade nanofluid towards the vertical surface was examined using an artificial neural network [17]. It should be noted that the microorganisms efficiently, which were suspended using a bio convection technique, stabilized the nanoparticles. Motivated by the growing interest in the topic of microorganisms, the present work operates in this direction.

An exponentially elongated surface was used to study the magneto-Darcy stream of a polarized nano liquid with Ohm's heat-up and viscous dissipation systems by numerical simulation [18]. The fourth-order Runge-Kutta (RK-4) based on shooting technique was utilized numerically to analyze the generated partial differential equations (PDEs) and to determine the significance of significant variables in physical characteristics. How Jeffrey fluid flowed across a vertical nonlinear stretchable surface of changing thickness was explored using an incompressible electro-magneto-hydrodynamic [19]. Numerous source terms, such as Jeffery dispersion, Ohmic heat up, thermophoretic, Brownian, temperature supply, temperature supply in exponential format, and activation force contributions, were considered while analyzing the impacts of mass and heat transmission. Several reliability parameters were computed taking into account various situations after the artificial neural networks and mixed model reliability requirements were examined [21]. An artificial neural network model with multiple layers was created to estimate the numerical reliability parameters that were acquired. It was looked at as a dependability model that used the artificial neural networks model and was based on the exponentiated Weibull distribution and the inverse power law model [22]. It was suggested how to use an artificial neural network with Bayesian regularization to create a generalized exponential distribution based on the inverse power law [23]. In a study conducted under reduced gravity, the impacts of substance rejoinder and varying viscosity on the oscillations of temperature and volume fractions transport over an inclining heating surface were investigated [24]. It was hypothetical that a fluid's viscosity varied with temperature. Consideration was given to the stream in two dimensions, where Navier-Stokes formulation with changing viscosity was considered [25]. The linear increased dissipation, close to the non-affine stationary states that the place of the Couette flows, was discovered. A thorough analysis was conducted of the effects of the flow and energy profile via a leaky tube with asymmetric cooling at the surfaces of dependent time, incompressible, third-grade liquid with reaction, and small electric conduction in addition to changeable viscosity [26]. An unstable MHD free convection flow of a micropolar liquid via a perpendicular cone-shaped with unfixed temperature fluctuation, viscous and Ohm dispersions was studied with the impacts of changeable stickiness and conduction of heat [27]. Inverse linear functions of temperature were used to represent the liquid stickiness and heat conductivity. A study was conducted on the bioconvective Jeffrey fluid, which transports small particles with varying thermal conductivity [28]. Diffusion theories proposed by Cattaneo-Christov were used to simulate mass and heat transfer. The flow was induced by the porous oscillating surface. An enhanced varied finite element technique of the Navier-Stokes form expressed in circumstances of pressure, speed, and vortices with unfixed viscosity and non-slip border criteria was examined [29]. The weak formulation contains terms derived from the constitutive equation and the incompressibility requirement, both of which are expressed as least squares. In light of nonlinear thermal radiation, the impact of heat-reliant stickiness and heat conduction on the extendable surface of a Powell-Eyring liquid was investigated [30].

In light of the aforementioned aspects, the present work is an attempt to scrutinize the border cover movement of non-Newtonian Sutterby nano-liquid comprising micro-organisms under the assumption of exponentially variable viscosity. The considered flow adjoins to a vertical extended sheet with the impact of Ohmic and non-Newtonian dissipations along with an exponentially-space heat source on heat exchange, besides nanomaterials distribution with chemical reactions. This model has a weighty contribution to similar models of stream owing to its numerous relevant implementations in engineering and manufacturing. There are lots of industrial processes related to the characteristics of flow across a distending cover. The impact of a variable viscosity depending on temperature, nanomaterial, and microbes' diffusions through a permeable region on a nano liquid flowing over a stretching wall plays a crucial role in the present problem. The procedure of several industries, such as various heat exchangers, food processing, fiber and wire coating, extrusion processes, polymer processing, and scheme of fusing metals, as an operative measurement. In jets, a thin polymer layer is also formed by the surrounding nano-fluid, creating an eternally dynamic plate with an irregular velocity that increases with space from the jet [16].

The foremost goal of the current analysis is to illustrate the behavior of the NSF containing microscopic beings in a permeable thin cover near a stretchable surface. Additionally, the influences of the variation of viscosity and normal magnetic direction on the progress are included. Finally, the effects of the relevant actual factors on the flow-structured profiles are shown. The significance of the current work is motivated by the microorganisms' involvement in temperature, velocity, and nanoparticle allocations to identify the advantages or disadvantages that nanoparticles and microorganisms such as bacteria, viruses, and microbes produce in the flow across surfaces. Furthermore, the dependence of viscosity on these relevant distributions gives more connotations to the study. The next sections of the article are arranged in such a way as to be followed easily. Also, the approach and relevant boundary conditions are illustrated together with the corresponding formulations of the stream and physical variables of significance. Moreover, the proper match conversions that convert the standard PDEs into ordinary differential equations (ODEs)



are discussed. In § 3, the numerical examination using the RK-4 with the shooting technique is presented. Physical reasons are accessible in § 4 to clarify the results. The primary observations and remarks are introduced in § 5.

## 2. Mathematical Formulations

The present investigation examines the two-dimensional steady incompressible non-Newtonian Sutterby nano liquid stream induced by a stretching wall. The structure is positioned to a uniform magnetic direction of force  $B_0$  which is perpendicular to the wall. The temperature energy is stressed by the Ohmic, non-Newtonian dissipations, and exponentially space-dependent heat source. Furthermore, the stream is concerned with the Brownian, thermophoretic features, and chemical activity. The novel aspect of the current analysis is the study of changeable viscosity that depends on the temperature, species concentration, and motile microorganisms. Applicable, it is assumed that the surface is conserved at fixed heat  $T_w$ , nanomaterials volume fractions  $C_w$  and microbes  $N_w$ , while they are assumed far from the wall to be  $T_\infty$ ,  $C_\infty$  and  $N_\infty$ . For a suitable structure, the Cartesian one is taken, where the co-axis of the stretching wall is the  $x$ -axis and  $y$  is the perpendicular axis. The surface wall is supposed to be stretching by speed  $u_w = ax$  such that  $a > 0$  is the stretching rate. This configuration is stressed and has been shown throughout Fig. 1(a). A very appropriate application of this paradigm is the air-vapor barrier, which facilitates the dispersion of moisture vapor by permitting it to flow through the tissues; see Fig. 1(b). Moreover, it stops the issues brought on by air seeping into structures.

Surface films or liquid-applied covers are two types of vapor-permeable air blockades. Variable permeability rates are offered by these kinds of barriers. Since our model has membranes that let mass, heat, and liquids travel through, this application could work well with it. With the use of nanoparticles and changing temperatures, the current study presents an amazing vision for heat transfer [16].

### 2.1. Main formulations

The covering formulae of the rheological state of the non-Newtonian Sutterby liquid may be demonstrated by Li et al. [31] as follows:

$$\underline{\tau} = -P\underline{I} + \underline{S}, \quad \underline{S} = \mu \left( \frac{\sinh^{-1} \Gamma \pi}{\Gamma \pi} \right)^m \underline{A}, \quad \text{and} \quad \pi = \sqrt{\frac{1}{2} \text{Trace}(\underline{A}^2)} \quad (1)$$

where  $\underline{A} = \nabla \underline{V} + \nabla \underline{V}^T$  signifies the Rivlin-Erickson matrix of first-order type,  $\underline{V} = (u, v, w)$  is the liquid speed,  $\Gamma$  is the characteristic time,  $m$  is the indicator of power law, and  $\mu$  is the liquid viscosity. Using the Taylor series, it can be said that  $\sinh^{-1} \Gamma \pi \approx \Gamma \pi - (\Gamma \pi)^3 / 3!$  as  $\Gamma \pi \ll 1$ , in which case the additional stress matrix [31] can be rewritten as:

$$\underline{S} = \mu \left( 1 - \frac{m \Gamma^2}{6} \pi^2 \right) \underline{A}. \quad (2)$$

Additionally, in contrast to previous studies that assumed that the fluid viscosity is constant with temperature [32], the current investigation takes into account that the nano liquid viscosity  $\mu$  may be comparative to heat  $T$ , nanomaterials fractions  $C$ , and microbes numbers  $N$  as follows:

$$\mu(T, C, N) = \mu_0 \exp[-(q_1(T - T_\infty) + q_2(C - C_\infty) + q_3(N - N_\infty))], \quad (3)$$

where,  $\mu_0$  is the constant viscosity. Further,  $q_1, q_2$  and  $q_3$  are dimensionless coefficients.

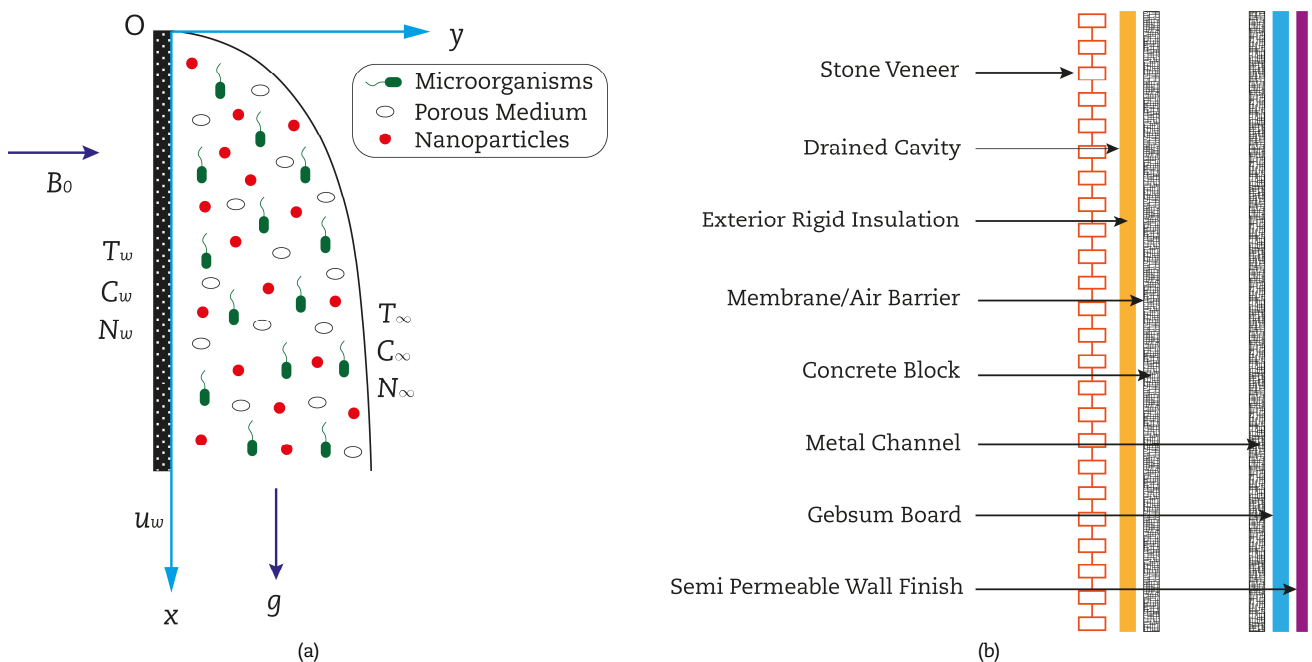


Fig. 1. (a) Graphical outline of the flow of the problem (b) Design and constituents of the air-vapor barrier.



The movement of the cooperative oxytactic microorganisms through the nano liquid may be introduced and formed mathematically by Patil et al. [33] as follows:

$$\frac{dN}{dt} = -\nabla \cdot \underline{\Sigma}, \text{ such that } \underline{\Sigma} = N\tilde{V} - D_m \nabla N \text{ and } \tilde{V} = \left( \frac{bW_c}{C_w - C_\infty} \right) \nabla C, \quad (4)$$

where  $\underline{\Sigma}$  signifies the microbes flux,  $\tilde{V}$  is the floating velocity average of microbes,  $D_m$  is the microbes dispersion which is assumed to be uniformly disseminated and constant in the fluid,  $W_c$  is the maximum velocity of the cell, and  $b$  is the chemotaxis factor.

Through these suppositions, taken into the description, the boundary layer theory of the governing stream formulae may be formulated respectively as follows:

Mass stability [34] gives:

$$\frac{\partial u}{\partial x} + \frac{\partial v}{\partial y} = 0, \quad (5)$$

Velocity in the stretching direction [34] is:

$$\rho_f \left( u \frac{\partial u}{\partial x} + v \frac{\partial u}{\partial y} \right) = \frac{\partial}{\partial y} \left[ \mu \left( \frac{\partial u}{\partial y} - \frac{m\Gamma^2}{6} \left( \frac{\partial u}{\partial y} \right)^3 \right) \right] - \left( \sigma B_0^2 + \frac{\mu}{k_1} \right) u + g \left[ \rho_f \beta' (1 - C_\infty) (T - T_\infty) - (\rho_p - \rho_f) (C - C_\infty) - \gamma (\rho_m - \rho_f) (N - N_\infty) \right], \quad (6)$$

where the last term refers to the bioconvective force that is dependent on temperature, species volume fractions, and microbes.

Energy conservation [34] becomes:

$$(\rho c)_f \left( u \frac{\partial T}{\partial x} + v \frac{\partial T}{\partial y} \right) = \alpha \frac{\partial^2 T}{\partial y^2} + (\rho c)_p \left[ D_b \frac{\partial T}{\partial y} \frac{\partial C}{\partial y} + \frac{D_T}{T_\infty} \left( \frac{\partial T}{\partial y} \right)^2 \right] + q_r (T - T_\infty) + q_e (T_w - T_\infty) e^{-y\sqrt{a/v}} + \sigma B_0^2 u^2 + \mu \left( 1 - \frac{m\Gamma^2}{6} \left( \frac{\partial u}{\partial y} \right)^2 \right) \left( \frac{\partial u}{\partial y} \right)^2, \quad (7)$$

where the last three terms refer to the contributions of temperature supply in exponentially – space, Ohmic, and Sutterby diffusion.

Species diffusion becomes [17, 35]:

$$u \frac{\partial C}{\partial x} + v \frac{\partial C}{\partial y} = D_b \frac{\partial^2 C}{\partial y^2} + \frac{D_T}{T_\infty} \frac{\partial^2 T}{\partial y^2} - R_1 (C - C_\infty), \quad (8)$$

such that the last term submits the material reaction and microbes density equation is [17,35]:

$$u \frac{\partial N}{\partial x} + v \frac{\partial N}{\partial y} + \frac{bW_c}{C_w - C_\infty} \frac{\partial}{\partial y} \left( N \frac{\partial C}{\partial y} \right) = D_m \frac{\partial^2 N}{\partial y^2}. \quad (9)$$

The stream of the current inspection is controlled by the above forms. A set of boundary restrictions should satisfy these forms. The appropriate border criteria [35] may be written as follows:

$$\left. \begin{aligned} u = u_w = ax, T = T_w, C = C_w, N = N_w \quad \text{at } y = 0 \\ u = 0, T = T_\infty, C = C_\infty, N = N_\infty \quad \text{as } y \rightarrow \infty \end{aligned} \right\}. \quad (10)$$

Now, the boundary-value problem of this investigation becomes clear. Section 4 demonstrates the solution approach.

## 2.2. Significant of physiological notations

The objective quantities of [13] required with the current article are the skin friction aspect  $C_f$ , the Nusselt quantity  $Nu$ , the Sherwood quantity  $Sh$ , and the Microbes measure  $Nn$  which can be formed as follows:

$$C_f = \mu \left( \frac{\partial u}{\partial y} - \frac{m\Gamma^2}{6} \left( \frac{\partial u}{\partial y} \right)^3 \right) \bigg|_{y=0} / \frac{1}{2} \rho_f a^2 x^2 \quad (11)$$

$$Nu = -x \frac{\partial T}{\partial y} \bigg|_{y=0} / (T_w - T_\infty) \quad (12)$$

$$Sh = -x \frac{\partial C}{\partial y} \bigg|_{y=0} / (C_w - C_\infty) \quad (13)$$

and

$$Nn = -x \frac{\partial N}{\partial y} \bigg|_{y=0} / (N_w - N_\infty) \quad (14)$$

## 2.3. Fitting similarity transformations

The dimensionless corresponding variables [32] are fittingly used to convert the PDEs (5) to (9) into ODEs. These variables can be spelled out as follows:



$$\psi = x\sqrt{av}f(\eta), \eta = y\sqrt{\frac{a}{v}}, \theta = \frac{T-T_\infty}{T_w-T_\infty}, \varphi = \frac{C-C_\infty}{C_w-C_\infty} \quad \text{and} \quad \chi = \frac{N-N_\infty}{N_w-N_\infty}, \quad (15)$$

where  $\psi$  is the stream function and  $\eta$  is the non-dimensional independent variable.

Equation (5) is similarly recognized considering associations (15), and the basic Eqs. (6) to (9) with the boundary constraints (10) can be stated using the following method:

$$\left(f''' - \frac{m}{2}\text{ReDe}f''^2f''' - (\beta_1\theta' + \beta_2\varphi' + \beta_3\chi')(f'' - \frac{m}{6}\text{ReDe}f''^3)\right)e^{-(\beta_1\theta + \beta_2\varphi + \beta_3\chi)} + Gr(\theta - Nr\varphi - Rb\chi) - \left(M + \frac{e^{-(\beta_1\theta + \beta_2\varphi + \beta_3\chi)}}{Da}\right)f' - f''^2 + ff'' = 0, \quad (16)$$

$$\theta'' + \text{Pr}\left(Nt\theta'^2 + Nb\theta'\varphi' + f\theta' + EcMf'^2 + Ec\left(1 - \frac{m}{6}\text{ReDe}f''^2\right)f'^2 + Q_T\theta + Q_Ee^{-\eta}\right) = 0, \quad (17)$$

$$\varphi'' + \frac{Nt}{Nb}\theta'' + Scf\varphi' - ScR\varphi = 0, \quad (18)$$

$$\chi'' - \text{Pe}(\chi'\varphi' + (\chi + \delta)\varphi'') + Lbf\chi' = 0, \quad (19)$$

with the border criteria:

$$\left. \begin{aligned} f = 0, f' = 1, \theta = \varphi = \chi = 1 \quad \text{at} \quad \eta = 0 \\ f', \theta, \varphi, \chi \rightarrow 0 \quad \text{as} \quad \eta \rightarrow \infty \end{aligned} \right\}. \quad (20)$$

In addition, in Eqs. (11) to (14), the physical interests might be reformulated as:

$$C_f = \frac{2}{\sqrt{\text{Re}}} \left( f''(0) - \frac{m}{6}\text{ReDe}f''^3(0) \right) e^{-(\beta_1\theta(0) + \beta_2\varphi(0) + \beta_3\chi(0))}, \quad (21)$$

$$Nu = -\sqrt{\text{Re}}\theta'(0), \quad (22)$$

$$Sh = -\sqrt{\text{Re}}\varphi'(0), \quad (23)$$

$$Nn = -\sqrt{\text{Re}}\chi'(0), \quad (24)$$

where  $\text{Re} = ax^2/v$  is the local Reynolds number.

For the sake of simplicity, it is appropriate to write all non-dimensional physical factors as:

$$Gr = g\beta^*(1 - C_\infty)(T_w - T_\infty)/a^2x, \quad Lb = v/D_m, \quad \delta = N_\infty/(N_w - N_\infty), \quad M = \sigma B_0^2/\rho_f a, \quad Rb = \gamma(\rho_m - \rho_f)(N_w - N_\infty)/\rho_f\beta^*(1 - C_\infty)(T_w - T_\infty),$$

$$De = a^2\Gamma^2, \quad \beta_1 = q_1(T_w - T_\infty), \quad \beta_2 = q_2(C_w - C_\infty), \quad \beta_3 = q_3(N_w - N_\infty), \quad \text{Pr} = \nu(\rho c)_f/\alpha, \quad Q_E = q_E/\rho c_f a, \quad Da = \rho_f a k_1/\mu_0,$$

$$Ec = a^2x^2/(T_w - T_\infty)c_f, \quad Q_T = q_T/\rho c_f a, \quad Sc = \nu/D_B, \quad R = R_1/a, \quad Nr = (\rho_p - \rho_f)(C_w - C_\infty)/\rho_f\beta^*(1 - C_\infty)(T_w - T_\infty),$$

$$Nb = (\rho c)_p D_B(C_w - C_\infty)/(\rho c)_f v, \quad Nt = (\rho c)_p D_T(T_w - T_\infty)/(\rho c)_f v T_\infty \quad \text{and} \quad \text{Pe} = bWc/D_m.$$

As a result, it should be emphasized that the ongoing analysis is a generalization of [32], as it is expressed by Eqs. (16) to (19) using the boundary criteria (20).

### 3. Numerical Approach

As previously seen, in the current study the basic equations are converted from a complex non-linear system into an ODE one using some appropriate transformations. The shooting process is utilized to reorganize the nonlinear ODEs (16) to (19) shared with the border conditions (20). Utilizing the two-point boundary-value problem RK-4 technique with Newton's reiteration, the current arrangement of ODEs is handled numerically [14, 36, 37]. Here, Mathematica software is used to support this approach. According to this numerical procedure, the step size  $10^{-2}$  has been selected, leading to error tolerance  $10^{-6}$ . The method steps can be settled as:

Firstly, Eqs. (16) to (19) may be modified as:

$$f''' = -\frac{1}{\left(1 - \frac{m}{2}\text{ReDe}f''^2\right)} \left( \left( Gr(\theta - Nr\varphi - Rb\chi) - Mf' - f''^2 + ff'' \right) e^{(\beta_1\theta + \beta_2\varphi + \beta_3\chi)} - \frac{1}{Da} f' - (\beta_1\theta' + \beta_2\varphi' + \beta_3\chi')(f'' - \frac{m}{6}\text{ReDe}f''^3) \right) \quad (25)$$

$$\theta'' = -\text{Pr} \left( Nt\theta'^2 + Nb\theta'\varphi' + f\theta' + EcMf'^2 + Ec\left(1 - \frac{m}{6}\text{ReDe}f''^2\right)f'^2 + Q_T\theta + Q_Ee^{-\eta} \right), \quad (26)$$

$$\varphi'' = -\frac{Nt}{Nb}\theta'' - Scf\varphi' + ScR\varphi, \quad (27)$$

$$\chi'' = \text{Pe}(\chi'\varphi' + (\chi + \delta)\varphi'') - Lbf\chi'. \quad (28)$$





Supposing the succeeding substitutions:

$$f = X_1, f' = X_2, f'' = X_3, \theta = X_4, \theta' = X_5, \varphi = X_6, \varphi' = X_7, \chi = X_8, \chi' = X_9, \quad (29)$$

then,

$$f''' = X_3', \theta'' = X_5', \varphi'' = X_7', \chi'' = X_9' \quad (30)$$

Equations (25) to (28) with the conditions (20) under the previous assumptions become:

$$X_3' = -\frac{1}{(1 - \frac{m}{2} \text{Re} De X_3^2)} \left( Gr(X_4 - Nr X_6 - Rb X_8) - M X_2 - X_2^2 + X_1 X_3 \right) e^{(\beta_1 X_4 + \beta_2 X_6 + \beta_3 X_8)} - \frac{1}{Da} X_2 - (\beta_1 X_5 + \beta_2 X_7 + \beta_3 X_9) \left( X_3 - \frac{m}{6} \text{Re} De X_3^3 \right), \quad (31)$$

$$X_5' = -Pr \left( Nt X_5^2 + Nb X_5 X_7 + X_1 X_5 + Ec M X_2^2 + Ec \left( 1 - \frac{m}{6} \text{Re} De X_3^2 \right) X_3^2 + Q_T X_4 + Q_E e^{-\eta} \right), \quad (32)$$

$$X_7' = -\frac{Nt}{Nb} X_5' - Sc X_1 X_7 + Sc R X_6, \quad (33)$$

$$X_9' = Pe(X_9 X_7 + (X_8 + \delta) X_7') - Lb X_1 X_9, \quad (34)$$

$$\left. \begin{aligned} X_1 = 0, X_2 = 1, \text{ and } X_4 = X_6 = X_8 = 1 \quad \text{at } \eta = 0 \\ X_2 \rightarrow 0, X_4 \rightarrow 0, X_6 \rightarrow 0 \text{ and } X_8 \rightarrow 0 \quad \text{as } \eta \rightarrow \infty \end{aligned} \right\} \quad (35)$$

Meanwhile, the circumstances (35) are insufficient to catch the solution of the combined Eqs. (31) to (34); therefore, before starting the solving procedure, an initial guesstimate for  $X_3(0), X_5(0), X_7(0), X_9(0)$  must be selected. The estimation domain  $[0, \eta_\infty]$  is taken instead of the real domain  $[0, \infty]$ , where  $\eta_\infty = 10$  is selected. The reiteration process is operated until the condition of convergence (the difference between the original boundary conditions in Eq. (20),  $f'(\infty) = \theta(\infty) = \varphi(\infty) = 0$ , and the calculated one is fewer than  $10^{-6}$  is satisfied; otherwise, the initial suppositions will be changed, see Fig. 2. The current approach is more accurate and simpler than the conventional RK-4 since it only uses two memory locations per dependent variable, as opposed to the traditional RK-4. This method works well for simulating linear wave phenomena.

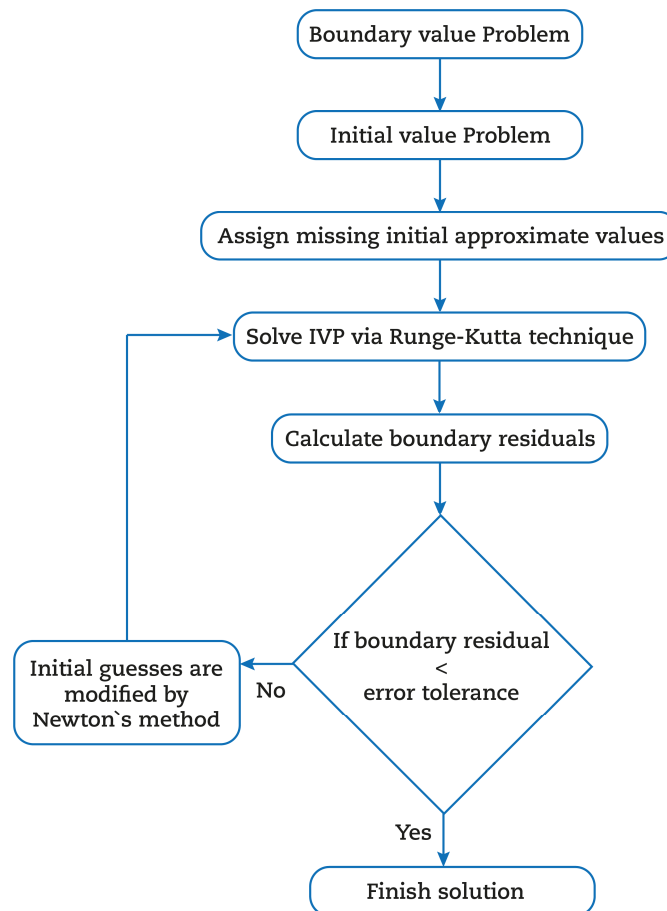


Fig. 2. Flowchart for the numerical approach.



**Table 1.** The horizontal nanofluid velocity  $f'$  calculations for the exact solution [38] and the current approach for different values of  $\eta$ .

$\eta$	Present numerical calculations	Exact solution [38]	Error
0.039	0.0386591476413136	0.0386593837529049	$2.3 \times 10^{-7}$
0.157	0.1453660783061044	0.1453678994115584	$1.8 \times 10^{-6}$
0.351	0.2960968776908371	0.2960990090423304	$2.1 \times 10^{-6}$
0.618	0.4612275832395130	0.4612300455246082	$2.4 \times 10^{-6}$
0.954	0.6151515852006927	0.6151551558484238	$3.5 \times 10^{-6}$
1.355	0.7420835325250135	0.7420931647336533	$9.6 \times 10^{-6}$

#### 4. Results and Discussion

The stream of an incompressible nanofluid comprising microorganisms and following the non-Newtonian Sutterby model is examined. The flow occupies the permeable region near a stretched sheet. The system lies under the impacts of a normal uniform magnetic field, Ohmic and non-Newtonian dissipations in addition to an exponential space-dependent heat source, and biochemical response. An exponential variable viscosity depending on temperature and concentrations of both nanoparticles and microbes is assumed. The current section clarifies the influences of many physical pertinent factors on the fluid speed trajectory, heat diffusion, nanoparticle capacity fraction, and microorganisms' concentration. Several drawings are plotted to attain a physical meaning of the influences of those control factors on the model overriding functions. The system (16) to (19) with boundary restrictions (20) are calculated numerically using the Runge-Kutta technique with the shooting approach via Mathematica 12 software. The evaluated outcomes are shown in figures and tables with fixed boundary layer thickness and a chosen sample system of proper particulars specified as:

$$\beta_1 = \beta_2 = \beta_3 = Nr = Rb = Gr = Q_T = Q_E \text{ Pe} = 0.1, Nb = 0.3, Nt = 0.05, Sc = \delta = Lb = 0.5, 0.8, Pr = 6.785,$$

$$Da = 1.4, M = 0.05, m = 0.1, Ec = 0.1, Re = 0.1, De = 0.1, \text{ and } \eta_\infty = 10.$$

##### 4.1. Velocity distribution

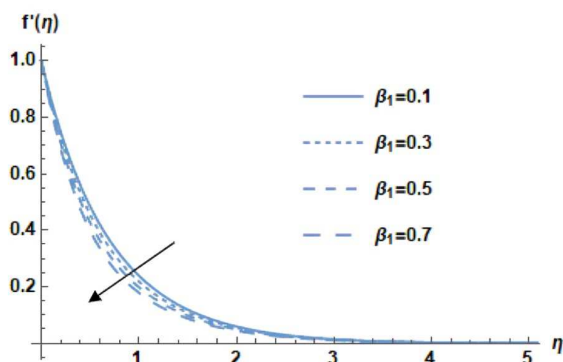
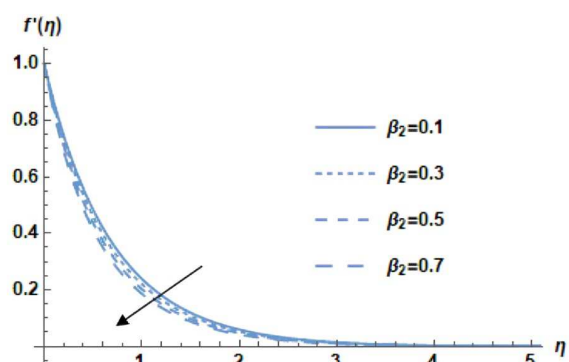
At the beginning of the discussion for the speed calculations, table 1 is designed to tabulate the current numerical solution of Eq. (16) for the horizontal speed  $f'$  in some special case where  $\beta_1 = \beta_2 = \beta_3 = m = M = Gr = 0$ , and  $Da \rightarrow \infty$ , as well as the exact solution that appears in [38]. The very small error between the present numerical solution and the exact one, that can be seen from the last column in Table 1, makes it potential to expand the calculated results.

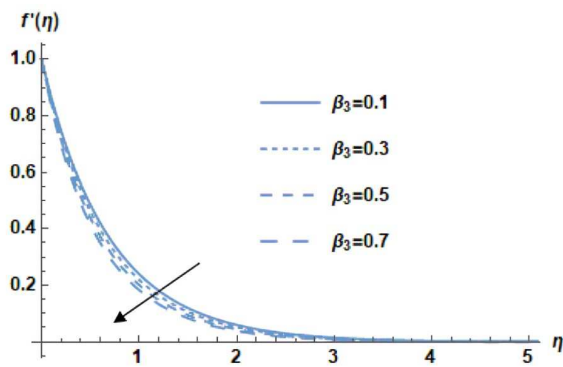
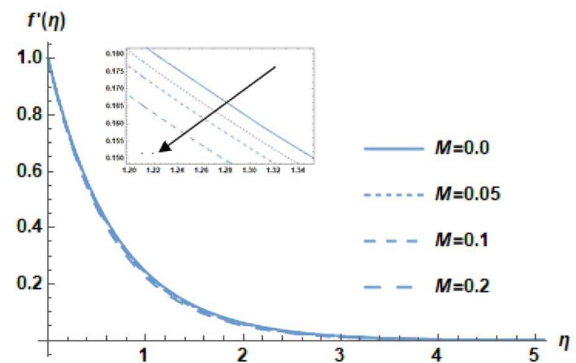
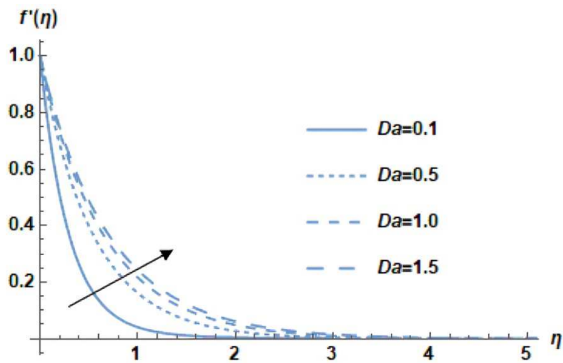
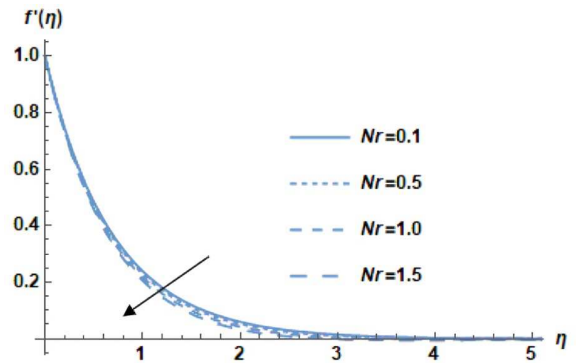
Figures 3 to 8 present the velocity schemes  $f'$  in comparison to the dimensionless variable  $\eta$ . These diagrams examine the influences of the viscosity variation parameters with temperature, nanoparticles, and microbes  $\beta_1, \beta_2, \beta_3$ , the magnetic element  $M$ , the Darcy factor  $K$  and the buoyancy ratio  $N_r$  on the speed dispersal  $f'$ .

Figures 3 to 5 indicate that the rise of all viscosity variation coefficients  $\beta_1, \beta_2, \beta_3$  decays the speed  $f'$ . Physically, the increase of those parameters raises the internal fluid's viscosity which in turn makes the flow more difficult and reduces its speed, as displayed in Figs. 3, 4, and 5. This result is in line with that first reported in [39, 40]. These outcomes reflect the effect of the viscosity dependence on temperature and nanoparticles/microorganisms concentration on the speed of the fluid flowing on the surface, which has many contributions to processes that deal with this type of flow, like paints and lubrication.

Figure 6 demonstrates that the flow speed declines with the growth of the magnetic coefficient  $M$ . Naturally, the reduction of  $f'$  owing to the increase of  $M$  results from the growth of the Lorentz force that obstructs the flow, and simultaneously drops the value of the stream speed. This numerical outcome accords with [41]. Moreover, Fig. 7 clarifies that the speed  $f'$  increases with the growth of the Darcy coefficient  $Da$ . From a physical standpoint, the Darcy numeral indicates the ratio between the penetrability of the medium and its cross-sectional area, so as  $Da$  rises, the permeability of the material advances, and the flow becomes easier. Consequently, the emergence  $Da$  leads to an intensification in the fluid movement. This conclusion is consistent with earlier research findings [42].

Figure 8 indicates that the speed  $f'$  drops with the increase of the buoyancy ratio  $N_r$ . For more usefulness, the buoyancy ratio is directly connected with the concentration of nanoparticles scattered in the fluid. Consequently, the variations of this parameter are associated with different kinds of these solid nanoparticles and identify their characteristics. The more gathering of these particles advances the resistance to the liquid flow and hence decays velocity. For more practicality, the buoyancy ratio is directly associated with the fluid's nanoparticle diffusion mediation. The increasing accumulation of these particles causes the fluid stream to become obstructed, which lowers the stream's velocity. This outcome corresponds to that obtained earlier in [12].

**Fig. 3.** The impact of  $\beta_1$  on the velocity  $f'(\eta)$ .**Fig. 4.** The impact of  $\beta_2$  on the velocity  $f'(\eta)$ .

Fig. 5. The impact of  $\beta_3$  on the velocity  $f'(\eta)$ .Fig. 6. The impact of  $M$  on the velocity  $f'(\eta)$ .Fig. 7. The impact of  $Da$  on the velocity  $f'(\eta)$ .Fig. 8. The impact of  $Nr$  on the velocity  $f'(\eta)$ .

#### 4.2. Temperature transmission distribution

Examination of heat transmutation is a very important requisite for inspecting and handling the liquid flows, particularly those associated with nanofluids classification. Therefore, Figs. 9 to 14 reveal the dimensionless temperature distribution  $\theta$  along with the dimensionless variable  $\eta$  to show the influences of the viscosity variation parameters on temperature  $\beta_1$ , the Brownian coefficient  $Nb$ , the linear and exponential heat source coefficients  $Q$  and  $Q_E$ , the Prandtl coefficient  $Pr$ , and the Eckert numeral  $Ec$ . It is found that all the effective parameters, except  $Pr$ , improved heat transmission which is an interesting and significant conclusion due to its importance in many applications.

The growth of temperature owing to the increase of the viscosity variation parameters with temperature, nanoparticles, and microbes  $\beta_1, \beta_2, \beta_3$  is demonstrated, but due to their similar effects and to avoid redundancy, only one figure representing the  $\beta_1$  impact will be concluded here, as seen in Fig. 9. As interpreted previously, the intensification of  $\beta_1, \beta_2, \beta_3$  means exponential growth of the internal viscosity and hence more friction between the fluid particles, which in turn creates a rise in fluid temperature and a progress in heat transmission, as shown in the chosen Fig. 9. This consequence is partially consistent with [40, 41]. Figure 10 illustrates the influence of the Brownian flow factor  $Nb$  on heat transmission. This figure shows that the augmentation of  $Nb$  enhances the liquid temperature and heat transmission. Naturally, the Brownian factor  $Nb$  is considered as a measure of the accidental moving nano-particles. Such movement raises heat in the closed zone of these very tiny particles leading to temperature escalation, as shown in Fig. 10. This deduction corresponds to that found by [11-16].

Figures 11 and 12 illustrate the influences of the linear and exponential heat resource measurements  $Q$  and  $Q_E$  on  $\theta$ . As seen from these figures, it is realized that energy grows with the growth of these two factors. Naturally, the augmentation in the heat source strictures signifies an essential cause of raising the inner temperature of the flow with any kind of heat source. Accordingly, supplementary sources of heat there are and the greater its coefficients, the higher the temperature of the flow. These findings are in accord with [43, 44]. Figure 13 confirms the drop in the temperature due to the growth of the Prandtl numeral  $Pr$  within the flow. Actually, the Prandtl coefficient  $Pr$  is a number that denotes the ratio between the momentum diffusivity and heat diffusivity. Furthermore,  $Pr$  represents the ratio between the fluid viscosity and the thermal conductivity, which indicates that as  $Pr$  rises, the thermal conductivity decays and hence the internal temperature losses, as concluded from Fig. 13. This consequence is consistent with that obtained earlier in [45].

The Eckert number  $Ec$  is found to be an intensifying factor of  $\theta$ , as shown in Fig. 14. In addition to indicating heat dissipation, the Eckert number  $Ec$  describes the relationship between the flow kinetic energy and the boundary layer enthalpy change. A rise in the basic liquid heat is one of the factors contributing to the temperature produced by heat dissipation of the relevant liquid particles. This outcome is consistent with earlier findings [11, 14]. The aforementioned findings show that heat transmission improves with almost all relevant factors, which is a useful conclusion for a number of applications, including reactors, hydraulic cylinders, and various forms of heat radiation treatment.

#### 4.3. Nanoparticles' volume fraction profiles

Figures 15 to 20 represent the nanoparticles' volume fraction  $\varphi$  versus the dimensions-free variable  $\eta$ . These figures indicate the impacts of the viscosity variation parameters with nanoparticles  $\beta_2$ , the thermophoretic constraint  $Nt$ , the Brownian contribution  $Nb$ , the bio convection Rayleigh numeral  $Rb$ , the Schmidt parameter  $Sc$ , and the chemical reaction stricture  $R$ , respectively. As mentioned in the temperature case, the three parameters  $\beta_1, \beta_2, \beta_3$  are similar in their influences, so it is sufficient





to discuss only one figure here. It is recognized from Fig. 15 that the nano-particle size fraction  $\varphi$  rises with the growth of  $\beta_2$ . From the abovementioned physical interpretation, the augmentation of these parameters improves viscosity which in turn leads to more accumulation of the included nano-particles and raises  $\varphi$ . For example, as seen in nature, this outcome finds an explanation in the accumulation of sugar granules as the viscosity of honey increases. Figure 16 demonstrates the influence of  $Nt$  on the  $\varphi$  supply, where it is found that  $\varphi$  increases with the rise of  $Nt$ . The growth of  $Nt$  means an improvement of the sheet temperature, which pushes the nanoparticles to more dispersal on the surface and raises  $\varphi$  in turn. This outcome accords with that of [46]. As remarked in Fig. 17,  $\varphi$  declines with the growth of the Brownian factor  $Nb$ . In fact, the growth of  $Nb$ , as an indicator of the accidental motion of nanomaterials, creates more divergence of the nanoparticles, which explains the lessening in nanoparticles concentration as illustrated by Fig. 17 and Ref. [47]. Figure 18 is plotted to illustrate the improvement impact of  $Rb$  on  $\varphi$ . The bio-convection Rayleigh number signifies the microorganisms' contribution to the buoyancy term. The increasing density of these microbes causes more of the nanomaterial to condense throughout the flow and improves its dispersion, as revealed by Fig. 18. This result agrees with that found in [48].

The growth of the Schmidt number  $Sc$  is found to be a rising factor of  $\varphi$ , as seen in Fig. 19. Essentially, the Schmidt number signifies the momentum-to-mass diffusivities ratio. Subsequently, mass diffusion declines with raising the quantities of  $Sc$ , which leads to a further congregation of particles and develops  $\varphi$ , as illustrated by Fig. 19. This finding agrees with that of [11, 49]. Figure 20 shows that as the chemical reactive element  $R$  increases, the nano-particle aggregation decreases. Physically, as  $R$  grows, an extensive dispersion of mass over the adjacent liquid arises. This result indicates that the combination of a nanoparticle's chemical activity results in decreased compression of these minuscule particles leading to more efficacy of nanoliquids' characteristics. Consequently, the growth of  $R$  leads to the distraction of nanoparticles within the flow, which reduces the nanoparticles' condensation. Furthermore, the chemical reaction is a resonance for improving heat, which causes more scattering of the dissolved particles along the flow, thus leading to a drop of  $\varphi$ , as determined from Fig. 20. This finding is in line with [12].

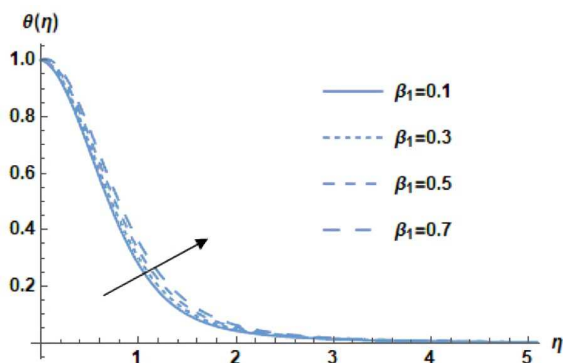


Fig. 9. The impact of  $\beta_1$  on the temperature  $\theta(\eta)$ .

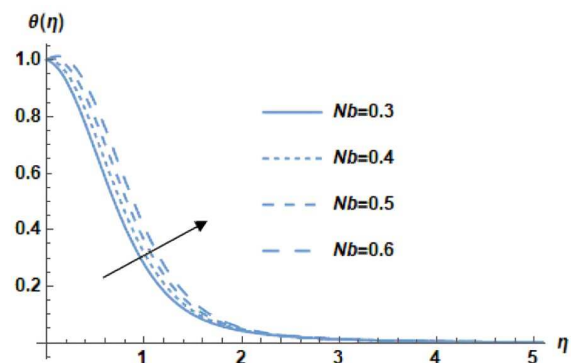


Fig. 10. The impact of  $Nb$  on the temperature  $\theta(\eta)$ .

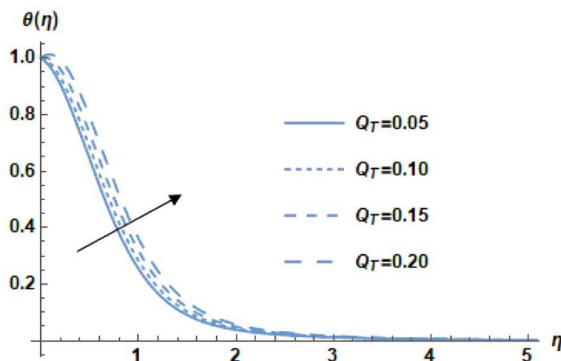


Fig. 11. The impact of  $Q_T$  on the temperature  $\theta(\eta)$ .

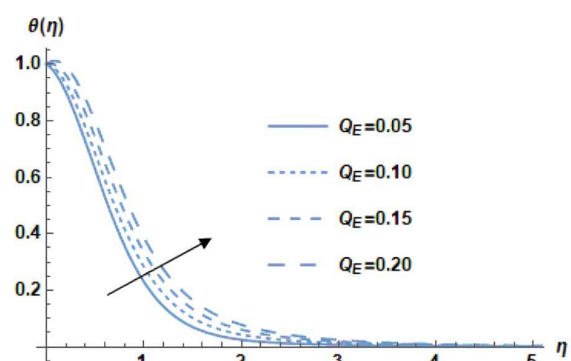


Fig. 12. The impact of  $Q_E$  on the temperature  $\theta(\eta)$ .

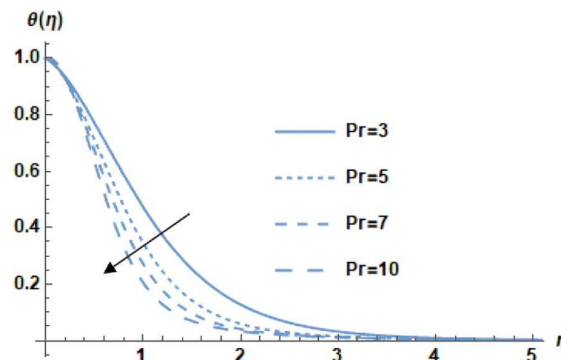


Fig. 13. The impact of  $Pr$  on the temperature  $\theta(\eta)$ .

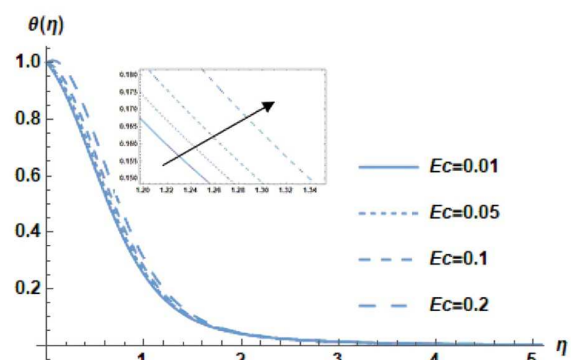
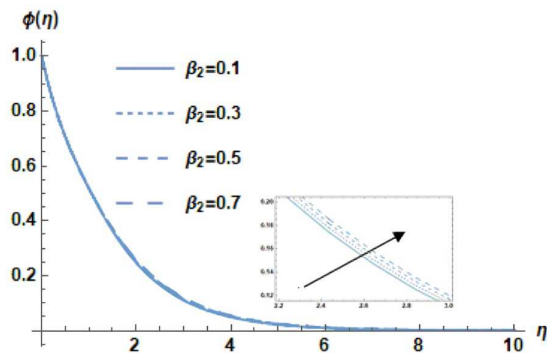
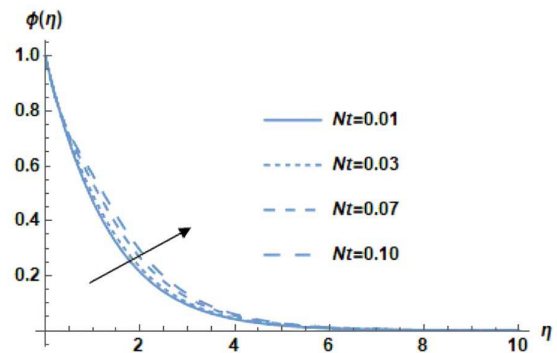
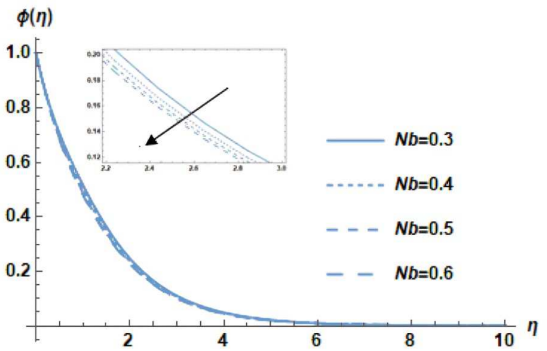
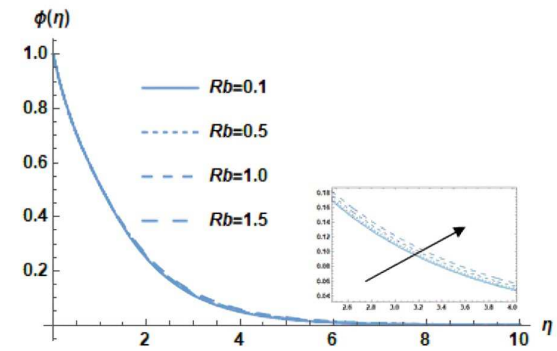
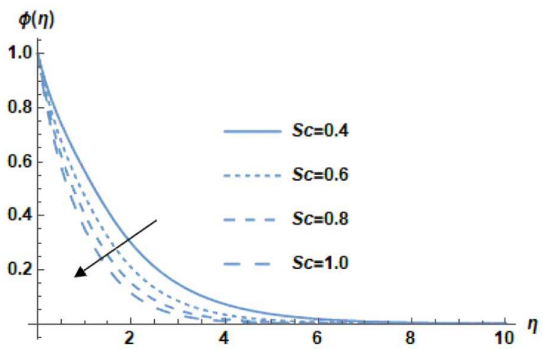
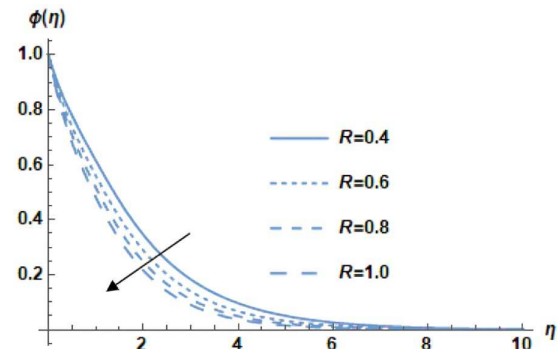


Fig. 14. The impact of  $Ec$  on the temperature  $\theta(\eta)$ .



Fig. 15. The impact of  $\beta_2$  on the nanoparticles concentration  $\varphi(\eta)$ .Fig. 16. The impact of  $Nt$  on the nanoparticles concentration  $\varphi(\eta)$ .Fig. 17. The impact of  $Nb$  on the nanoparticles concentration  $\varphi(\eta)$ .Fig. 18. The impact of  $Rb$  on the nanoparticles concentration  $\varphi(\eta)$ .Fig. 19. The impact of  $Sc$  on the nanoparticles concentration  $\varphi(\eta)$ .Fig. 20. The impact of  $R$  on the nanoparticles concentration  $\varphi(\eta)$ .

#### 4.4. Microorganisms concentration distribution

Figures 21 to 26 display the distribution of microorganisms  $\chi$  versus  $\eta$  to signify the influences of the viscosity variation parameter with microbes  $\beta_3$ , the buoyancy ratio factor  $Nr$ , the Peclet numeral  $Pe$ , the bioconvection constant  $\delta$ , the Lewis numeral  $Lb$ , and the bioconvection Rayleigh numeral  $Rb$ . As obtained before and given the similarity of the viscosity variation constants effect, it suffices to review only one of these effects, say  $\beta_3$ . Therefore, Fig. 21 represents the impact of  $\beta_3$  on the  $\chi$  profile. It is recognized that  $\beta_3$  as well as  $\beta_1$  and  $\beta_2$  are growing factors for microbes' existence. Actually, the growth of these strictures improves viscosity which, sequentially, leads to more gathering of the included microorganisms and raises these floating organisms. Figure 22 shows that the profile of microbes diminishes with the growth of  $Pe$ . Considerably,  $Pe$  indicates the proportion of the heat dissipation resulting from fluid streaming to that resulting from heat conductivity. Consequently, the augmentation of  $Pe$  indicates a growth in temperature, which is reflected in a larger scattering rate of microorganisms, creating a reduction of  $\chi$ , as indicated by Fig. 22. This conclusion is compatible with an earlier one [50]. Moreover, Fig. 23 specifies that  $\chi$  declines with the growth of  $Lb$ . Materially,  $Lb$  is identified as the proportion between heat and mass diffusion coefficients. Accordingly,  $Lb$  causes a reduction in the microbes' concentration  $\chi$ . This effect accords with that reported before in [51, 52].

As a depiction of the buoyancy terms impacts on  $\chi$ , Figs. 24 and 25 indicate that the  $\chi$  profile improves with the rise of  $Nr$  and  $Rb$ . These figures show that the aggregation of microbes improves with the growth of the buoyancy element  $Nr$  along with the bio convection Rayleigh numeral  $Rb$ . Naturally, these buoyancy coefficients are directly proportional to the concentrations of the dispersed nanoparticles and microorganisms through the liquid flow. This is a logical reason to raise both  $\chi$  and  $\varphi$ . Finally, Fig. 26 signifies the influence of the bio convection constant  $\delta$  on the microbes' dispersal  $\chi$ . As shown from this figure, the microorganism accumulation declines with the growth of  $\delta$ . Bioconvection conformations are frequently noticed in experiments for low arbitrary interruptions of swaying microbes which have less compactness than water as a pure liquid. Consequently, the rise of the bio convection constant  $\delta$  means less aggregation of these microorganisms, as indicated by Fig. 26. This conclusion accords with an early finding reported in [15, 53]. The abovementioned results can be useful in predicting which parameters lead to enhancing or eliminating the presence of these microbes, bacteria, and viruses. The aforementioned results can be helpful in identifying the parameters that, when increased or decreased, aid in the removal of hazardous bacteria, germs, and organisms from the pointed surface.



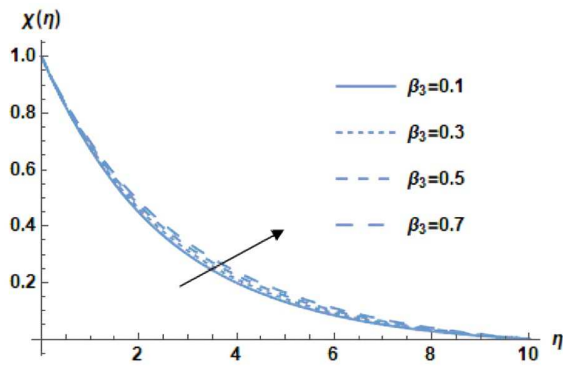


Fig. 21. The impact of  $\beta_3$  on the microbes concentration  $\chi(\eta)$ .

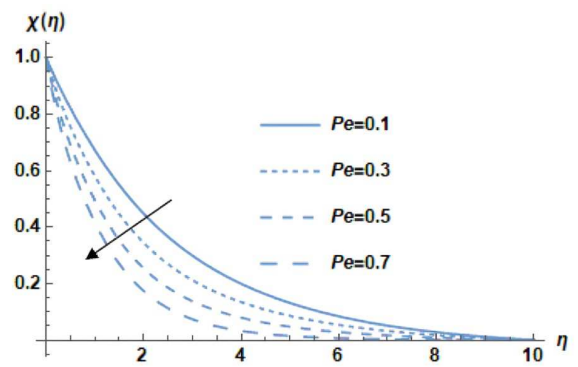


Fig. 22. The impact of  $Pe$  on the microbes concentration  $\chi(\eta)$ .

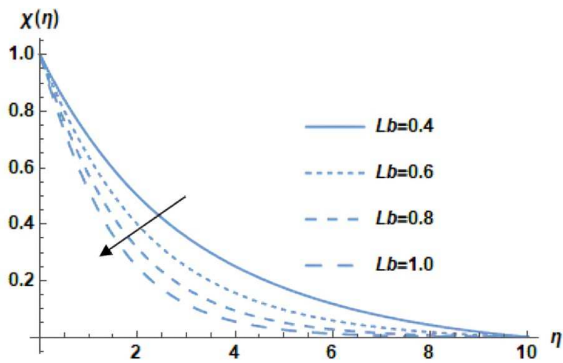


Fig. 23. The impact of  $Lb$  on the microbes concentration  $\chi(\eta)$ .

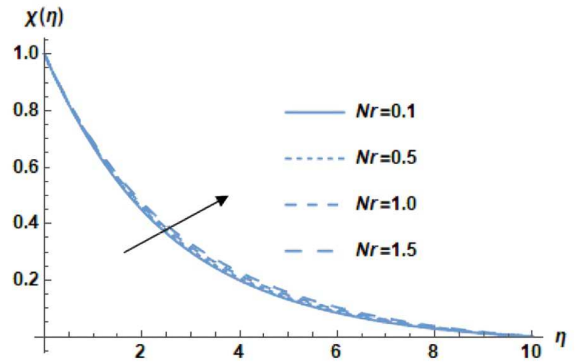


Fig. 24. The impact of  $Nr$  on the microbes concentration  $\chi(\eta)$ .

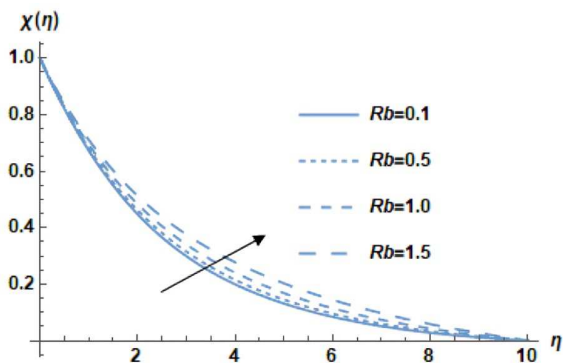


Fig. 25. The impact of  $Rb$  on the microbes concentration  $\chi(\eta)$ .

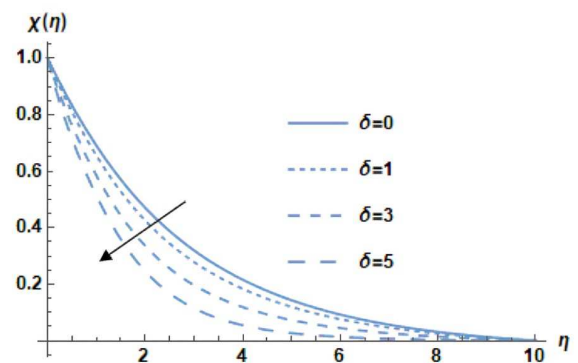


Fig. 26. The impact of  $\delta$  on the microbes concentration  $\chi(\eta)$ .

Table 2. The behavior of  $Cf$ ,  $Nu$ ,  $Sh$  and  $Nn$  for various values of  $\beta_1, \beta_2, \beta_3$ .

$\beta_1$	$\beta_2$	$\beta_3$	$f''(0)$	$-\theta'(0)$	$-\varphi'(0)$	$-\chi'(0)$
0.1	0.1	0.1	-6.87350	0.02525100	0.246627	0.126149
		0.3	-6.11201	0.00182738	0.248821	0.123351
		0.5	-5.41270	-0.0238333	0.251337	0.120564
		0.7	-4.77368	-0.0517678	0.254188	0.117829
0.1	0.1		-6.87350	0.02525100	0.246627	0.126149
	0.3		-6.12530	0.00487664	0.248513	0.123547
	0.5		-5.46128	-0.0173899	0.250689	0.121024
	0.7		-4.87140	-0.0416445	0.253178	0.118612
	0.1	0.1	-6.87350	0.02525100	0.246627	0.126149
		0.3	-6.06473	0.00542873	0.248412	0.123415
		0.5	-5.35537	-0.0163551	0.250485	0.120736
		0.7	-4.73298	-0.0402443	0.252875	0.118148



**Table 3.** The behavior of  $C_f$ ,  $Nu$ ,  $Sh$  and  $Nn$  for various values of  $m$ ,  $Re$  and  $De$ .

$m$	$Re$	$De$	$f''(0)$	$-\theta'(0)$	$-\varphi'(0)$	$-\chi'(0)$
0.1	0.1	0.1	-6.87350	0.02525100	0.246627	0.126149
	0.5		-6.87066	0.02518390	0.246629	0.126133
	1		-6.86710	0.0250996	0.246631	0.126112
	2		-6.85995	0.0249296	0.246636	0.126070
0.1	0.1		-6.87350	0.02525100	0.246627	0.126149
	0.5		-3.07265	0.0563129	0.551479	0.282041
	1		-2.17157	0.0793719	0.779916	0.398800
	2		-1.53393	0.1114890	1.102990	0.563802
	0.1	0.01	-6.87414	0.025266	0.246627	0.126153
		0.03	-6.87399	0.0252627	0.246627	0.126152
		0.05	-6.87385	0.0252593	0.246627	0.126151
		0.08	-6.87364	0.0252543	0.246627	0.126150

**Table 4.** Comparative analysis for  $f''(0)$  at  $\beta_1 = \beta_2 = \beta_3 = m = M = Gr = 0$  and  $Da \rightarrow \infty$ .

$M$	Hayat et al. [54]	Li et al. [55]	Present numerical outcomes
0.0	-1.000000	-1.000000	-1.0000083735820064
0.5	-1.224747	-1.224748	-1.2247449166155746
1.5	-1.581147	-1.581149	-1.5811388300982105
2.0	-1.732057	-1.7320577	-1.7320580075694827

#### 4.5. Skin friction, Nusselt, Sherwood, and Motile factors

Tables 2 and 3 illustrate the amounts of the skin friction factor  $f''(0)$ , Nusselt  $-\theta'(0)$ , Sherwood  $-\varphi'(0)$  and Motile  $-\chi'(0)$  numbers. Table 2 indicates the estimated values of  $f''(0)$ ,  $-\theta'(0)$ ,  $-\varphi'(0)$  and  $-\chi'(0)$  against the variations of the variable viscosity parameters  $\beta_1, \beta_2, \beta_3$ . It can be noted that those three factors have similar influences, whether increasing or decreasing, on the current physical quantities. Furthermore, Table 3 represents the same coefficient values with the variation of  $m$ ,  $Re$  and  $De$ . These estimations give significant indicators about velocity, heat, nanoparticles, and motile microbes fluxes at the expanding reference wall.

Finally, Table 4 provides a comparison between the values of  $f''(0)$  estimated from the current work in the special case,  $\beta_1 = \beta_2 = \beta_3 = m = M = Gr = 0$ , and  $Da \rightarrow \infty$ , and those evaluated in earlier studies [54, 55]. The current numerical results and the ones approximated by [54, 55] are found to be in good agreement.

## 5. Conclusion

Owing to the wide range of industries that use stretching sheets and surfaces for industrial processes, jets, and polymers, this study provides a valuable understanding of this significant field of research. The present study investigates the numerical solution method of an incompressible Sutterby nano-liquid motion resulting from a stretched wall that suspends gyrotactic microorganisms. The liquid passes through a permeable medium under the influence of a homogenous vertical MF, while the nanomaterials transmission is accessible through chemical interaction. The temperature spread is determined by Ohmic and non-Newtonian dissipations in addition to exponentially-space heat source. The novelty of the current analysis comes from considering the exponentially changing viscosity versus temperature, nanomaterial, and Microbes' diffusions. Additionally, the involvement of the microbes in the flow also gives the current work more significance due to its extensive applicable fields, especially those affected by the variation of liquid viscosity. Changes in viscosity, such as those brought on by changes in temperature or species composition, are frequently a defining characteristic of turbulent flows in engineering and environmental applications. The mathematical construction of the problem has been outlined with proper similarity alterations which have been utilized to convert the overriding PDEs to ODEs. Several non-dimensional physical quantities have been considered and proven to be important factors in the current various major distributions. As a result, a series of graphs and numerical tables have been designed to demonstrate how the relevant elementary factors might be inferred. Utilizing the shooting technique and the RK-4 framework, a numerical analysis has been conducted using Mathematica Software 12.0 to generate flow-specific nature distributions of the distinctive main functions of temperature, velocity, concentrations of nanoparticles, and microorganisms. Research on heat diffusion, diffusion thermos effects, rotation, homogeneous and heterogeneous chemical reactions, and several other non-Newtonian fluid categories may be considered as open points for the current work.

The major findings of the current work can be summarized in these points:

- The improvement of velocity distribution is contingent upon the medium's increasing permeability. Simultaneously, it declines with the growth of the viscosity variation parameters with temperature, nanoparticles, microbes, the magnetic element, and the heat buoyancy ratio.
- Heat diffusion declines only with the growth of the Prandtl coefficient, while it improves with the rise of all the other relevant factors, which is thought to be an important phenomenon associated with the presence of nanoparticles.
- Nanoparticles size fraction drop off with the rise of the Brownian, Schmidt, and biochemical strictures. Simultaneously, it improves with the growth of viscosity variation, thermophoresis, and bio-convection Rayleigh coefficients and in turn advances the temperature, which is a significant outcome that can be esteemed in several applications.
- Microbes accumulation is found to increase with the intensification of the viscosity variation, the buoyancy ratio, and the bioconvection Rayleigh coefficients. Moreover, it is found to decrease with the growth of the Peclet, the Lewis, and the



bioconvection constants. These findings may be useful in expecting the enhancement and reducing factors of these microscopic organisms.

- Numerical analysis and comparison with prior research using a range of parametric values have been conducted for the skin friction, Nusselt, nano-Sherwood, and motile coefficients.

### Author Contributions

G.M. Moatimid supervised and administered the project; N.S. Elgazery applied the numerical approach, plotted the data; M.A.A. Mohamed analyzed the numerical outcomes and conceptualized the physical issue; K. Elagamy made a mathematical suggestion and created a mathematical model. The manuscript was written through the contribution of all authors. All authors contributed to the writing of the manuscript. The final version of the article was reviewed by all authors, who also gave their approval.

### Acknowledgments

The reviewers' insightful observations, supportive remarks, and helpful recommendations to enhance the original article are all greatly appreciated by the authors.

### Conflict of Interest

Regarding the research, writing, and/or publication of this work, the authors declared that there were no potential conflicts of interest.

### Funding

The authors have no financial support for the authorship, work, and/or publication of the current manuscript.

### Data Availability Statements

The datasets generated and/or analyzed during the current study are available from the corresponding author on reasonable request.

### Nomenclature

#### English Symbols

$\underline{I}$	Unit tensor
$\underline{\underline{S}}$	Extra stress tensor
$\underline{\underline{A}}$	Rivlin Erickson tensor
$k_1$	Permeable factor
$g$	Gravity acceleration
$D_b$	Brownian diffusivity
$D_T$	Thermophoretic diffusion
$q_T$	Thermal source factor
$q_E$	Exponential thermal source factor
$R_1$	Substance reaction
$De$	Deborah factor
$Gr$	Grashof contribution
$Rb$	Bio convection contribution
$Da$	Darcy factor
$M$	Magnetic contribution
$Pr$	Prandtl contribution
$Nt$	Thermophoretic factor
$Sc$	Schmidt number
$Ec$	Eckert number
$Q_T$	Dimensionless thermal source factor
$Q_E$	Dimensionless exponential thermal source factor
$Pe$	Peclet numeral
$Lb$	Lewis numeral
$Nr$	Buoyancy ratio numeral

#### Greek Symbols

$\nu$	Kinematic viscosity
$\alpha$	Thermal conductivity
$\rho_f$	Fluid density
$\beta^*$	Volumetric extension factor
$\rho_p$	Density of nanoparticles
$\rho_m$	Density of microbes
$\gamma$	Microorganisms average volume
$(\rho c)_f$	Temperature capacity of the liquid
$(\rho c)_p$	Heat capacity of the nanomaterials
$\sigma$	Electrical conductivity
$\beta_1$	Non-dimensional exponential temperature factor
$\beta_2$	Non-dimensional exponential nano materials factor
$\beta_3$	Non-dimensional exponential microbes factor
$\delta$	Bio-convection constant
$\theta$	Non-dimensional heat
$\varphi$	Non-dimensional nanoparticles
$\chi$	Non-dimensional microbes





## References

- [1] Sohail, M., Nazir, U., Chu, Y.M., Alrabaiah, H., Al-Kouz, W., Thounthong, P., Computational exploration for radiative flow of Sutterby nanofluid with variable temperature dependent thermal conductivity and diffusion coefficient, *Open Physics*, 18, 2020, 1073–1083.
- [2] Imran, N., Javed, M., Sohail, M., Thounthong, P., Abdelmalek, Z., Theoretical exploration of thermal transportation with chemical reactions for Sutterby fluid model obeying peristaltic mechanism, *Journal of Materials Research and Technology*, 9(4), 2020, 7449–7459.
- [3] Fayyadh, M.M., Naganthran, K., Basir, M.F.M., Hashim, I., Roslan, R., Radiative MHD sutterby nanofluid flow past a moving sheet: scaling group analysis, *Mathematics*, 8, 2020, 1–17.
- [4] Hayat, T., Ahmad, S., Khan, M.I., Alsaedi, A., Modeling chemically reactive flow of sutterby nanofluid by a rotating disk in presence of heat generation/absorption, *Communications in Theoretical Physics*, 69, 2018, 1–8.
- [5] Saif-ur-Rehman, Mir, N.A., Farooq, M., Rizwan, M., Ahmad, F., Ahmad, S., Ahmad, B., Analysis of thermally stratified flow of Sutterby nanofluid with zero mass flux condition, *Journal of Materials Research and Technology*, 9(2), 2020, 1631–1639.
- [6] Nawaz, M., Role of hybrid nanoparticles in thermal performance of Sutterby fluid, the ethylene glycol, *Physica A: Statistical Mechanics and its Applications*, 537, 2020, 1–10.
- [7] Waqas, H., Farooq, U., Bhatti, M.M., Hussain, S., Magnetized bioconvection flow of Sutterby fluid characterized by the suspension of nanoparticles across a wedge with activation energy, *ZAMM Journal of Applied Mathematics and Mechanics*, 101, 2021, 1–19.
- [8] El-Dabe, N.T.M., Moatimid, G.M., Mohamed, M.A.A., Mohamed, Y.M., A couple stress of peristaltic motion of Sutterby micropolar nanofluid inside a symmetric channel with a strong magnetic field and Hall currents effect, *Archive of Applied Mechanics*, 91, 2021, 3987–4010.
- [9] Bijiga, L.K., Gamachu, D., Neural network method for quadratic radiation and quadratic convection unsteady flow of Sutterby nanofluid past a rotating sphere, *SN Applied Sciences*, 5(49), 2023, 1–15.
- [10] Arain, M.B., Zeeshan, A., Bhatti, M.M., Mohammed, Sh. Alhodaly, M.Sh., Ellahi, R., Description of non-Newtonian bioconvective Sutterby fluid conveying tiny particles on a circular rotating disk subject to induced magnetic field, *Journal of Central South University*, 30, 2023, 2599–2615.
- [11] Moatimid, G.M., Mohamed, M.A.A., Elagamy, K., A motion of Jeffrey nanofluid in porous medium with motile microorganisms between two revolving stretching discs: Effect of Hall currents, *Journal of Porous Media*, 25(10), 2022, 83–10.
- [12] Moatimid, G.M., Mohamed, M.A.A., Elagamy, K., Peristaltic transport of Rabinowitsch nanofluid with moving microorganisms, *Scientific Reports*, 13, 2023, 1–21.
- [13] Moatimid, G.M., Mohamed, M.A.A., Elagamy, K., A pulsatile Williamson nanofluid flow with motile microorganisms between two permeable walls: Effect of modified Darcy's law, *Journal of Porous Media*, 26(12), 2023, 57–86.
- [14] He, J.H., Moatimid, G.M., Mohamed, M.A.A., Elagamy, K., A stretching cylindrical Carreau nanofluid border layer movement with motile microorganisms and variable thermal characteristics, *International Journal of Modern Physics B*, 2023, DOI: 10.1142/S0217979224502230.
- [15] Moatimid, G.M., Mohamed, M.A.A., Elagamy, K., Microorganisms peristaltic transport within a Carreau nanofluid through a modified Darcy porous medium, *Special Topics and Reviews in Porous Media*, 14(5), 2023, 1–30.
- [16] Moatimid, G.M., Mohamed, M.A.A., Elagamy, K., A Williamson nanofluid with motile microorganisms across a vertical exponentially stretching porous sheet with varying thermal characteristics, *Special Topics and Reviews in Porous Media*, 15(1), 2024, 67–98.
- [17] Shafiq, A., Çolak, A.B., Sindhu, T.N., Development of an intelligent computing system using neural networks for modeling bioconvection flow of second-grade nanofluid with gyrotactic microorganisms, *Numerical Heat Transfer, Part B: Fundamentals*, 2023.
- [18] Rana, P., Mahanthesh, B., Nisar, K.S., Swain, K., Devi, M., Boundary layer flow of magneto-nanomicroscopic liquid over an exponentially elongated porous plate with Joule heating and viscous heating: A numerical study, *Arabian Journal for Science and Engineering*, 46, 2021, 12405–12415.
- [19] Sharma, R.K., Kumar, A., Gandhi, R., M.M. Bhatti, Exponential space and thermal-dependent heat source effects on electro-magneto-hydrodynamic Jeffrey fluid flow over a vertical stretching surface, *International Journal of Modern Physics B*, 36(30), 2022, 1–19.
- [20] Mahanthesh, B., Shashikumar, N.S., Gireesha, B.J., Animasaun, I.L., Effectiveness of Hall current and exponential heat source on unsteady heat transport of dusty TiO<sub>2</sub>-EO nanoliquid with nonlinear radiative heat, *Journal of Computational Design and Engineering*, 6(4), 2019, 551–561.
- [21] Shafiq, A., Çolak, A.B., Lone, S.A., Sindhu, T.N., Muhammad, T., Reliability modeling and analysis of mixture of exponential distributions using artificial neural network, *Mathematical Methods in the Applied Sciences*, 2022, 1–21.
- [22] Shafiq, A., Çolak, A.B., Sindhu, T.N., Reliability investigation of exponentiated Weibull distribution using IPL through numerical and artificial neural network modeling, *Quality and Reliability Engineering International*, 38, 2022, 3616–3631.
- [23] Sindhu, T.N., Çolak, A.B., Lone, S.A., Shafiq, A., Reliability study of generalized exponential distribution based on inverse power law using artificial neural network with Bayesian regularization, *Quality and Reliability Engineering International*, 39(6), 2023, 2398–2421.
- [24] Ullah, Z., Alkinidri, M., Effect of variable viscosity on oscillatory heat and mass transfer in mixed convective flow with chemical reaction along inclined heated plate under reduced gravity, *Alexandria Engineering Journal*, 77, 2023, 539–552.
- [25] Liao, X., Zillinger, C., On variable viscosity and enhanced dissipation, *Nonlinearity*, 36(11), 2023, 6071–6103.
- [26] Padhi, S., Nayak, I., Variable viscosity effects on unsteady MHD reactive third-grade fluid with asymmetric convective cooling within porous Couette device, *International Journal of Ambient Energy*, 44(1), 2023, 2422–2432.
- [27] Hazarika, G.C., Phukan, B., Ahmed, S., Effect of variable viscosity and thermal conductivity on unsteady free convective flow of a micropolar fluid past a vertical cone, *Journal of Engineering Physics and Thermophysics*, 93, 2020, 178–185.
- [28] Kolsi, L., Al-Khaled, K., Khan, S.U., Khedher, N.B., Effect of thermal radiation and variable viscosity on bioconvective and thermal stability of non-Newtonian nanofluids under bidirectional porous oscillating regime, *Mathematics*, 11, 2023, 1–18.
- [29] Anaya, V., Caraballo, R., Ruiz-Baier, R., Torres, H., On augmented finite element formulation for the Navier--Stokes equations with vorticity and variable viscosity, *Computers & Mathematics with Applications*, 143, 2023, 397–416.
- [30] Sarkar, A., Mondal, H., Nandkeolyar, R., Powell-Eyring fluid flow over a stretching surface with variable properties, *Journal of Nanofluids*, 12, 2023, 47–54.
- [31] Li, S., Khan, M. I., Alruqi, A.B., Khan, S.U., Abdullaev, S.S., Fadhil, B.M., Makhdoum, B.M., Entropy optimized flow of Sutterby nanomaterial subject to porous medium: Buongiorno nanofluid model, *Heliyon*, 9, 2023, 1–16.
- [32] He, J.H., Elgazery, N.S., Elagamy, K., Abd Elazem, N.Y., Efficacy of a modulated viscosity- dependent temperature /nanoparticles concentration parameter on a nonlinear radiative electromagneto nanofluid flow along an elongated stretching sheet, *Journal of Applied and Computational Mechanics*, 9(3), 2023, 848–860.
- [33] Patil, P.M., Goudar, B., Patil, M., Momoniat, E., Bioconvective periodic MHD Eyring-Powell fluid flow around a rotating cone: Influence of multiple diffusions and oxytactic microorganisms, *Alexandria Engineering Journal*, 81, 2023, 636–655.
- [34] Bilal, S., Shah, I.A., Akgül, A., Tekin, M.T., Botmart, T., Yousef, E., Yahia, I.S., A comprehensive mathematical structuring of magnetically effected Sutterby fluid flow immersed in dually stratified medium under boundary layer approximations over a linearly stretched surface, *Alexandria Engineering Journal*, 61, 2022, 11889–11898.
- [35] Alharbi, K.A.M., Farooq, U., Waqas, H., Imran, M., Noreen, S., Akgül, A., Baleanu, D., El Din, S.M., Abbas, K., Numerical solution of Maxwell-Sutterby nanofluid flow inside a stretching sheet with thermal radiation, exponential heat source/sink, and bioconvection, *International Journal of Thermofluids*, 18, 2023, 1–9.
- [36] Afify, A.A., Elgazery, N.S., Effect of chemical reaction on magnetohydrodynamic boundary layer flow of Maxwell fluid over a stretching sheet with nanoparticles, *Particuology*, 29, 2016, 154–161.
- [37] Elgazery, N.S., Nanofluids flow over a permeable unsteady stretching surface with non-uniform heat source/sink in the presence of inclined magnetic field, *Journal of the Egyptian Mathematical Society*, 27(9), 2019, 1–26.
- [38] Eldabe, N.T., Elshehawey, E.F., Elbarbary, E.M.E., Elgazery, N.S., Chebyshev finite difference method for MHD flow of a micropolar fluid past a stretching sheet with heat transfer, *Applied Mathematics and Computation*, 160, 2005, 437–450.
- [39] Manjunatha S., Gireesha B.J., Effects of variable viscosity and thermal conductivity on MHD flow and heat transfer of a dusty fluid, *Ain Shams Engineering Journal*, 7, 2016, 505–515.
- [40] Chauhan S.S., Shah P.D., Tiwari A., Analytical Study of the Effect of Variable Viscosity and Heat Transfer on Two-Fluid Flowing through Porous Layered Tubes, *Transport in Porous Media*, 142, 2022, 641–668.
- [41] Ibrahim W., Magnetohydrodynamics (MHD) flow of a tangent hyperbolic fluid with nanoparticles past a stretching sheet with second order slip



and convective boundary condition, *Results in Physics*, 7, 2017, 3723–3731.

[42] Arthur, E.M., Seini, I.Y., Bortteir, L.B., Analysis of Casson Fluid Flow over a Vertical Porous Surface with Chemical Reaction in the Presence of Magnetic Field, *Journal of Applied Mathematics and Physics*, 3(6), 2015, 713–723.

[43] Pal, D., Mandal, G., Double diffusive magnetohydrodynamic heat and mass transfer of nanofluids over a nonlinear stretching/shrinking sheet with viscous-Ohmic dissipation and thermal radiation, *Propulsion and Power Research*, 6(1), 2017, 58–69.

[44] Majeed, A., Javed, T., Mustafa, I., Ghaffari, A., Heat transfer over a stretching cylinder due to variable prandtl number influenced by internal heat generation/absorption: a numerical study, *Revista Mexicana de Física*, 62, 2016, 317–324.

[45] El-Dabe, N.T.M., Moatimid, G.M., Mohamed, M.A.A., Mohamed, Y.M., A couple stress of peristaltic motion of Sutterby micropolar nanofluid inside a symmetric channel with a strong magnetic field and Hall currents effect, *Archive of Applied Mechanics*, 91(9), 2021, 3987–4010.

[46] Abdul Halim, N., Noor, N.F.M., Mixed convection flow of Powell–Eyring nanofluid near a stagnation point along a vertical stretching sheet, *Mathematics*, 9, 2021, 1–17.

[47] Misra, S., Govardhan, K., Influence of chemical reaction on the heat and mass transfer of nanofluid flow over a nonlinear stretching sheet: A numerical study, *International Journal of Applied Mechanics and Engineering*, 25(2), 2020, 103–121.

[48] Kotnurkar, A.Sh., Katagi, D.C., Bioconvective peristaltic flow of a third-grade nanofluid embodying gyrotactic microorganisms in the presence of Cu-blood nanoparticles with permeable walls, *Multidiscipline Modeling in Materials and Structures*, 17(2), 2021, 293–316.

[49] Khan, M.I., Qayyum, S., Hayat, T., Stratified flow of Sutterby fluid with homogeneous-heterogeneous reactions and Cattaneo-Christov heat flux, *International Journal of Numerical Methods for Heat and Fluid Flow*, 29(8), 2019, 2977–2992.

[50] Khan, N.M., Abidi, A., Khan, I., Alotaibi, F., Alghtani, A.H., Aljohani, M.A., Galal, A.M., Dynamics of radiative Eyring–Powell MHD nanofluid containing gyrotactic microorganisms exposed to surface suction and viscosity variation, *Case Studies in Thermal Engineering*, 28(4), 2021, 1–16.

[51] Waqas, H., Farooq, U., Muhammad, T., Hussain, S., Khan, I., Thermal effect on bioconvection flow of Sutterby nanofluid between two rotating disks with motile microorganisms, *Case Studies in Thermal Engineering*, 26, 2021, 1–15.


[52] Elbashbeshy, E.M., Asker, A.G., Nagy, B., The effects of heat generation absorption on boundary layer flow of a nanofluid containing gyrotactic microorganisms over an inclined stretching cylinder, *Ain Shams Engineering Journal*, 13, 2022, 1–14.


[53] Balla, Ch.Sh., Alluguvelli, R., Naikoti, K., Makinde, O.D., effect of chemical reaction on bioconvective flow in oxytactic microorganisms suspended porous cavity, *Journal of Applied and Computational Mechanics*, 6(3), 2020, 653–664.


[54] Hayat, T., Mustafa, M., Pop, I., Heat and mass transfer for Soret and Dufour's effect on mixed convection boundary layer flow over a stretching vertical surface in a porous medium filled with a viscoelastic fluid, *Communications in Nonlinear Science and Numerical Simulation*, 15, 2010, 1183–1196.


[55] Li, S., Khan, M.I., Alruqi, A.B., Khan, S.U., Abdullaev, S.S., Fadhl, B.M., Makhdoum, B.M., Entropy optimized flow of Sutterby nanomaterial subject to porous medium, Buongiorno nanofluid model, *Heliyon*, 9(7), 2023, 1–15.

## ORCID iD

Galal M. Moatimid  <https://orcid.org/0000-0001-6833-8903>

Nasser S. Elgazery  <https://orcid.org/0000-0003-4691-2526>

Mona A.A. Mohamed  <https://orcid.org/0000-0003-3338-260X>

Khaled Elagamy  <https://orcid.org/0000-0001-8216-3935>



© 2024 Shahid Chamran University of Ahvaz, Ahvaz, Iran. This article is an open access article distributed under the terms and conditions of the Creative Commons Attribution-NonCommercial 4.0 International (CC BY-NC 4.0 license) (<http://creativecommons.org/licenses/by-nc/4.0/>).

**How to cite this article:** Moatimid G.M., Elgazery N.S., Mohamed M.A.A., Elagamy K. Bio-Convection Flow of Sutterby Nanofluid with Motile Microbes on Stretchable Sheet: Exponentially Varying Viscosity, *J. Appl. Comput. Mech.*, 10(3), 2024, 488–502. <https://doi.org/10.22055/jacm.2024.45527.4380>

**Publisher's Note** Shahid Chamran University of Ahvaz remains neutral with regard to jurisdictional claims in published maps and institutional affiliations.

